Fuzzy Bio-Interface: Logicality of Living Neuronal Network and Control of Fuzzy Bio-Robot System

I.Hayashi
Kansai University
Takatsuki, Osaka, Japan
ihaya@cbii.kutc.kansai-u.ac.jp

M.Kiyotoki
Kansai University
Takatsuki, Osaka, Japan
remora0909@yahoo.co.jp

A.Kiyohara
Kwansei Gakuin University
and Osaka University
Hyogo and Osaka, Japan
ai-kiyohara@kwansei.ac.jp

M.Tokuda
Kwansei Gakuin University
Sanda, Hyogo, Japan
m.tokuda@kwansei.ac.jp

S.N.Kudoh
Kwansei Gakuin University
Sanda, Hyogo, Japan
snkudoh@kwansei.ac.jp

***Abstract*— Rat hippocampal neurons are organized into complex networks in a culture dish with 64 planar microelectrodes. Multi-site recording system for extracellular action potentials is used for recording the activity of living neuronal networks and for applying input from the outer world to the network. The living neuronal network is able to express several patterns independently, and that's meaning that it has fundamental mechanisms for intelligent information processing. In this paper, we propose a significant algorithm to analyze logicality and connectivity of electrodes in a culture dish, and show the fuzzy bio-robot we developed. We control a robot by describing several characteristic of living neuronal network in fuzzy rules. We call it fuzzy bio-interface. Fuzzy bio-interface consists of two kinds of fuzzy logic to translate stimulus of living neuronal network from sensor signal of robot, and control action of robot from response of living neuronal network. We discuss the usefulness of fuzzy bio-interface using some examples.**

I. INTRODUCTION

Rat hippocampal neurons are organized into complex networks in a culture dish with 64 planar microelectrodes. Multi-site recording system for extracellular action potentials is used for recording the activity of living neuronal networks [1] and for applying input from the outer world to the network. The living neuronal network is able to express several patterns independently, and that's meaning that it has fundamental mechanisms for intelligent information processing [2]. Bettencourt et al. [3] classify the connectivity of action potentials of three electrodes on multi-site recording system by entropy and discussed the characteristic of each classification. However, they have not argued any time change of the connectivity of the action potential of the electrode.

In this paper, we propose a significant algorithm to analyze logicality and connectivity of electrodes in a culture dish, and show the fuzzy bio-robot we developed [4]. First, we discuss how to extract the logicality from living neuronal network in vitro with fuzzy $t-norm$ and $t-conorm$ operators [5]. Next, we control a robot by describing several characteristic of living neuronal network in fuzzy rules [6]–[10]. We call it "fuzzy bio-interface". Tsukamoto [11] has argued fuzzy interface in which fuzzy sets is regarded as a useful tool to intermediate between language and mathematics. Robot systems controlled by a living neuronal network are proposed by Potter et al. [12], Chao et al. [13], and Warwick et al. [14]. DeMarse et al. have proposed a flight simulation by living neuronal network [15]. Other examples are found in [16], [17]. However, these systems connect living neural network and outside world robot simply, and achieve no learning function, and no purposely-designed mechanism in a robot. We show a robot system controlled by a living neuronal network and fuzzy bio-interface. Fuzzy bio-interface consists of two kinds of fuzzy logic to translate stimulus of living neuronal network from sensor signal of robot, and control action of robot from response of living neuronal network. We estimated the learning of living neuronal networks with an example of straight running with fuzzy bio-robot [18]. From the results, we conclude that the logicality of neuronal networks and the adaptability of the fuzzy interface work efficiently.

II. NEURON CULTURE AND MULTI-ELECTRODE ARRAY

The conduct of all experimental procedures was governed by The Animal Welfare, Care and Use Committee in AIST. The hippocampus neurons were prepared from a Wister rat on embryonic day 17-18 (E17-18) and cultured by the previously described method [2]. Briefly, neurons were dissociated by treatment with 0.175% trypsin (Gibco, U.S.A.) and cultured by plating 500,000 cells in a $7mm$ diameter-glass ring on poly-D-lysine coated MED probe (Alpha MED Sciences, Japan), which has 64 planar placed microelectrodes. The medium is based on D-MEM/F12, supplemented with 5% horse serum (Gibco, U.S.A.) and 5% fetal calf serum (Gibco, U.S.A.).

This work was partially supported by the Ministry of Education, Culture, Sports, Science, and Technology of Japan under Grant-in-Aid for Scientific Research 18500181, 19200018, and 18048043, and the Organization for Research and Development of Innovative Science and Technology (ORDIST) of Kansai University.

The field action potentials were recorded 10-100days after the start of the culture. The spontaneous action potentials (sAPs) were gathered with the MED64 system (Alpha MED Sciences, Japan) at a 10-20 kHz sampling rate. Evoked field action potentials (eAPs) at 62 sites in the cultured networks were recorded with the MED64 system at a 20 kHz sampling rate. All experiments were carried out at room temperature ($20-25°$). The recorded spikes were detected by our developing program, sorted and classified by the amplitude versus decay time distributions using k-means cluster cutting method and converted to event trains.

III. Fuzzy Connective Operators

The fuzzy connective operators consists of $t-norm$ and $t-conorm$ operators. $t-norm$ T is a projective function expressed by $T(x,y)\ :\ [0,1]\times[0,1]\ \rightarrow\ [0,1]$, which satisfies four conditions, id est, boundary conditions, monotonicity, commutativity and associativity. $t-norm$ operator includes logical product, algebraic product, bounded product and drastic product. $t-conorm$ operator S is dual function of $t-norm$ operator, which is expressed by $S(x,y)\ :\ [0,1]\times[0,1]\rightarrow[0,1]$, and includes logical sum, algebraic sum, bounded sum and drastic sum.

On the other hand, many parametric $t-norm$ and $t-conorm$ operators have been proposed. By changing the values of parameter, the parametric fuzzy operator expresses the drastic $t-norm$ to the drastic $t-conorm$. For example, the parametric fuzzy operator proposed by Schweizer [5] is expressed as follows:

$$\begin{aligned} T(x,y) &= 1-((1-x)^{p_n}+(1-y)^{p_n} \\ &\quad -(1-x)^{p_n}(1-y)^{p_n})^{1/p_n} \qquad (1) \\ S(x,y) &= (x^{p_c}+y^{p_c}-x^{p_c}y^{p_c})^{1/p_c} \qquad (2) \end{aligned}$$

where, p_n and p_c are parameters.

By changing values of the parameter p_n and p_c, the Schweizer $t-norm$ and $t-conorm$ express logical operator ($p=\infty$), algebraic operator ($p=1$) and drastic operator ($p=0$).

IV. Acquisition of Logicality in Neuronal Networks

For discussing logicality of neuronal networks, we detected action potentials provided as pulse-time series for $120s$ with $20Hz$ at 64 electrodes. We selected an arbitrary set of three electrodes x,y,z, and analyzed the coherence pattern between the three electrodes. Now, we divide the data of pulse-time series in several time-bins, and set delay deviation between time-bins of two electrodes. The proposed algorithm is shown in Figure 1. In the electrode z as output elctrode, we detect a fuzzy set of the pulse frequency, F_i^z, in the i-th time-bin by the following membership function with center a_i^z and width c_i^z.

$$a_i^z = \frac{p_i^z - sp^z}{lp^z - sp^z} \qquad (3)$$

$$c_i^z = |a_i^z - E(a_i^z)| \qquad (4)$$

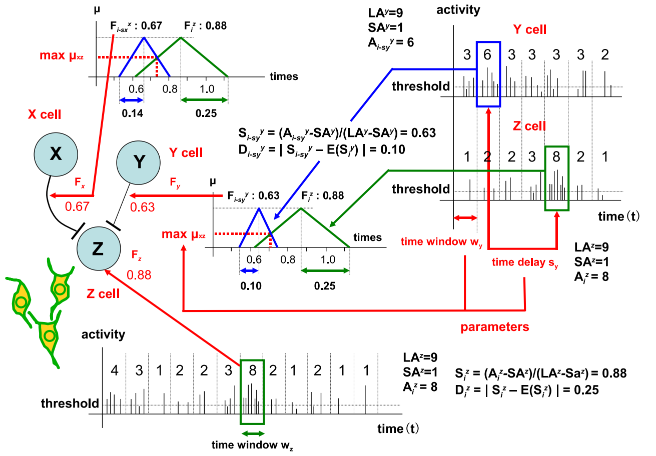

Fig. 1. Algorithm for Analysis of Action Potentials in Cultured Neuronal Network

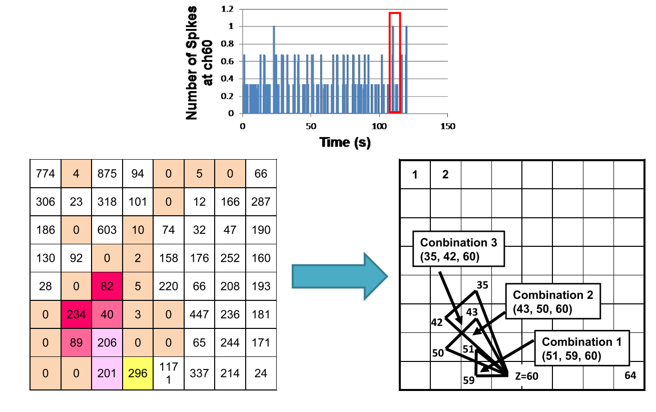

774	4	875	94	0	5	0	66
306	23	318	101	0	12	166	287
186	0	603	10	74	32	47	190
130	92	0	2	158	176	252	160
28	0	82	5	220	66	208	193
0	234	40	3	0	447	236	181
0	89	206	0	0	65	244	171
0	0	201	296	117 1	337	214	24

(A) Number of Spikes **(B) Location of Three Electrodes**

Fig. 2. Experiments

where, p_i^z is the number of pulse in the i-th time-bin, sp^z and lp^z are the minimum and maximum number of p_i^z, respectively. $E(a_i^z)$ is the average value of a_i^z.

The membership function $F_{i-s_x}^x$ with the delay deviation s_x is calculated in the electrode x as the input elctrode as same as the electrode z. Our purpose is to let the degree of coincidence, μ_{xz}^*, between F_i^z and $F_{i-s_x}^x$ maximize on the time x. To let the degree of coincidence maximize, the width of time-bin w_x and the delay deviation s_x are adjusted. We denote the adjusted pair of the width of time-bin and the delay deviation by $Opt(w_x^*, s_x^*)$.

$$\mu_{xz} = \sup_t \ \mu_{F_i^z}(t) \wedge \mu_{F_{i-s_x}^x}(t) \qquad (5)$$

$$Opt(w_x^*, s_x^*) = \max_{w_x, s_x} \ \mu_{xz}. \qquad (6)$$

We adjust the pair of $Opt(w_y^*, s_y^*)$ between the electrode y and the electrode z.

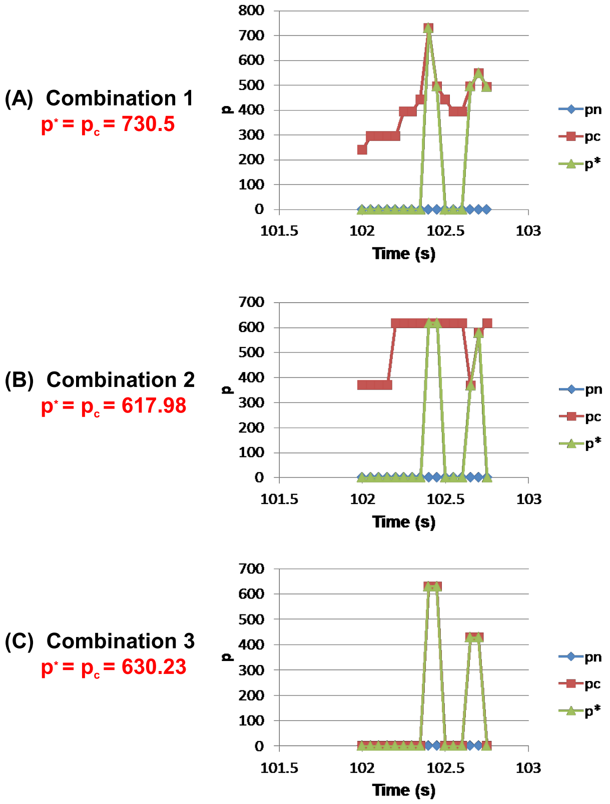

Fig. 3. Analysis of Action Potentials

TABLE I

EXAMPLES OF ELECTRODE ANALYSIS

Time Bin	1	2	3	4	5	6	7	8	9	10
Experiment 1										
X	2	3	2	**2**	0	1	3	1	3	1
Z	0	0	1	3	1	**2**	0	0	0	0
CofX	0.67	1.0	0.67	**0.67**	0.0	0.33	1.0	0.33	1.0	0.33
WofX	0.067	0.4	0.067	**0.067**	0.6	0.27	0.4	0.27	0.4	0.27
CofZ						**0.33**				
WofZ						**0.27**				
μ	1.0	0.6	1.0	**1.0**	0.36	0.52	0.6	0.52	0.6	0.52
Experiment 2										
X	2	3	2	0	0	1	0	1	**3**	1
Z	0	0	1	0	0	**2**	0	0	0	1
CofX	0.67	1.0	0.67	0.0	0.0	0.33	0.0	0.33	**1.0**	0.33
WofX	0.23	0.57	0.23	0.43	0.43	0.1	0.43	0.1	**0.57**	0.1
CofZ						**0.33**				
WofZ						**0.8**				
μ	0.68	1.0	0.68	0.19	0.19	0.26	0.19	0.26	**1.0**	0.26
Experiment 3										
X	0	1	0	2	0	**1**	0	2	0	0
Z	0	0	1	2	3	**1**	0	0	0	0
CofX	0.0	0.5	0.0	0.1	0.0	**0.5**	0.0	0.1	0.0	0.0
WofX	0.3	0.2	0.3	0.7	0.3	**0.2**	0.3	0.7	0.3	0.3
CofZ						**0.33**				
WofZ						**0.1**				
μ	0.17	0.44	0.17	0.17	0.17	**0.44**	0.17	0.17	0.17	0.17

Next, we calculate the output of the Schweizer operator with two centers of membership functions, $a^{x}_{i-s_x}$ of the electrode x and $a^{y}_{i-s_y}$ of the electrode y, respectively.

$$T(x,y) = 1-((1-a^{x}_{i-s_x})^{p_n}+(1-a^{y}_{i-s_y})^{p_n} -(1-a^{x}_{i-s_x})^{p_n}(1-a^{y}_{i-s_y})^{p_n})^{1/p_n} \quad (7)$$

$$S(x,y) = ((a^{x}_{i-s_x})^{p_c}+(a^{y}_{i-s_y})^{p_c} -(a^{x}_{i-s_x})^{p_c}(a^{y}_{i-s_y})^{p_c})^{1/p_c}. \quad (8)$$

We adjust the parameter p_n of $t-norm$ and the parameter p_c of $t-conorm$ to minimize a deviation between the center a^{z}_{i} of the electrode z and the Schweizer output, and select the solution parameter p^* from either p_n or p_c to minimize the deviation.

$$p^* = \{p_n, p_c | \min_{p_n,p_c}(|T(x,y)-a^{z}_{i}|,\ |S(x,y)-a^{z}_{i}|)\}. \quad (9)$$

To illustrate the proposed algorithm, we show a simple numerical example. The spike frequency of three combinations of electrodes x and z are shown in Table I and Figures 4 to 6. In each combination, we searched which spike of x electrode coincides with the spike frequency of time-bin 6 of electrode z by the proposed algorithm. In the first example, we estimated that the spike frequency "2" of time-bin 4 of electrode x coincides with the spike frequency "2" of time-bin 6 of electrode z with the degree $\mu^{*}_{xz} = 1.0$ of fuzzy sets.

Figures 4 shows the result of the first example. In the second and third examples, we estimated the spike frequency "3"of time-bin 9 and the spike frequency "1" of time-bin 6 coincide with the spike frequency "2" with $\mu^{*}_{xz} = 1.0$ and the spike frequency "1" $\mu^{*}_{xz} = 0.44$ of time-bin 6 of electrode z, as shown in Figures 5 and Figures 6.

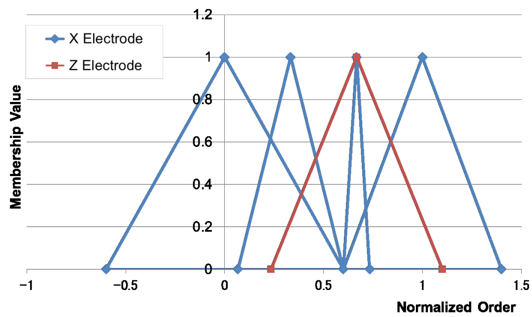

Fig. 4. Fuzzy Sets of the First Example of Electrode Analysis

For tangible data analysis, we selected three sets of input electrodes from 63 electrodes because of the output in the 60th electrode ($60el$). Figure 2 shows the location of three combinations of the input and output electrodes. In $60el$, we detected the sudden increasing of pulse frequency at $102.4s$ after the pulse frequency drastically decreased to 6

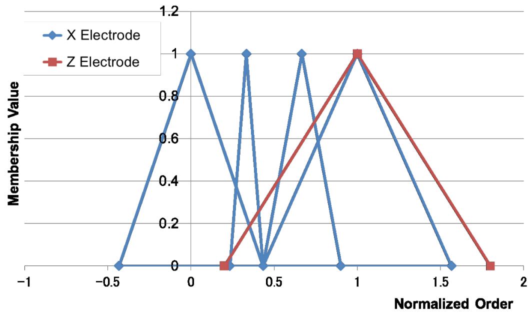

Fig. 5. Fuzzy Sets of the Second Example of Electrode Analysis

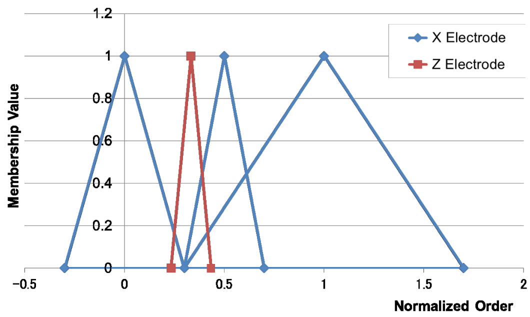

Fig. 6. Fuzzy Sets of the Third Example of Electrode Analysis

times at the around $95s$. For the analysis, we focus this characteristic pulse increasing at $102.4s$, and analyzed how this characteristic pulse influenced it for the following three combinations.

1. A combination of $(x, y, z) = (51el,\ 59el,\ 60el)$
2. A combination of $(x, y, z) = (43el,\ 50el,\ 60el)$
3. A combination of $(x, y, z) = (35el,\ 42el,\ 60el)$

The result is shown in Figure 3. We showed the degree of coincidence between membership functions μ^*_{xz} and μ^*_{yz}, and the optimum parameter values of fuzzy operators p^*, p_n and p_c. In the first combination of electrodes $(x, y, z) = (51el, 59el, 60el)$, the maximum degrees of coincidence are adjusted as $\mu^*_{xz} = 0.85$, $\mu^*_{yz} = 0.75$ with $w_x = 11s$, $w_y = 10s$, and the optimum parameter of Schweizer operator is converged to $p^* = p_c = 730.5$. In the second combination of electrodes $(x, y, z) = (43el, 50el, 60el)$, the maximum degrees of coincidence are adjusted $\mu^*_{xz} = 1.0$, $\mu^*_{yz} = 1.0$ with $w_x = 11s$, $w_y = 10s$, and the optimum parameter of Schweizer operator is converged to $p^* = p_c = 617.98$. In the third combination of electrodes $(x, y, z) = (35el, 42el, 60el)$, the maximum degrees of coincidence are adjusted as $\mu^*_{xz} = 0.76$, $\mu^*_{yz} = 0.91$ with $w_x = 11s$, $w_y = 10s$, and the optimum parameter of Schweizer operator is converged to $p^* = p_c = 630.23$. From these results, we conclude that the characteristic pulse increasing in $60el$ at $102.4s$ propagates to $(51el, 59el) \rightarrow (43el, 50el) \rightarrow (35el, 42el)$. And then, the parameters of Schweizer operator have been converged to $p^* = p_c = 730.5$ in $(51el, 59el)$, $p^* = p_c = 617.98$ in $(43el, 50el)$, and $p^* = p_c = 630.23$ in $(35el, 42el)$. These parameters mean logical sum. However, we should notice that the parameter of Schweizer operator at around $102.4s$ is $p^* = p_n = 0.0$, which means the drastic product. Therefore, despite all of our intuition, we conclude that the logicality of electrodes became to drastically change to weak OR relation from strong AND relation when a crowd of the pulses was fired and the pulse propagated distantly and widely.

V. Fuzzy Bio-Robot System

Fuzzy bio-robot includes two kinds of fuzzy logic units as fuzzy bio-interface, that is FLTD and FLBU. The FLTD, Fuzzy Logic unit in Top Down, is located in top-down processing, and infers the rotation speed of robot actuator from the pattern of action potential in multi-electrode array. The FLBU, Fuzzy Logic unit in Bottom Up, is located in bottom-up processing, and infers the electrical stimulation points in multi-electrode array from output values of robot sensors. Figure 7 explains the relationship between living neuronal networks and robot, and Figure 8 shows the concept of fuzzy bio-robot system.

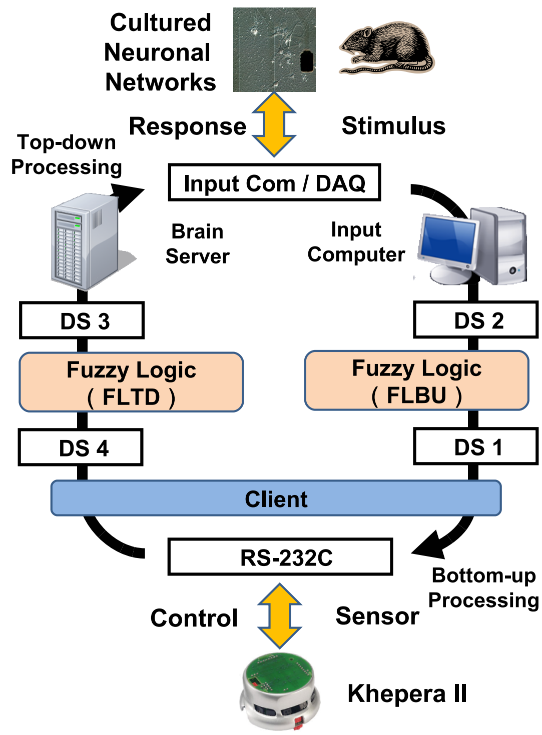

Fig. 7. Living Neuronal Network and Robot

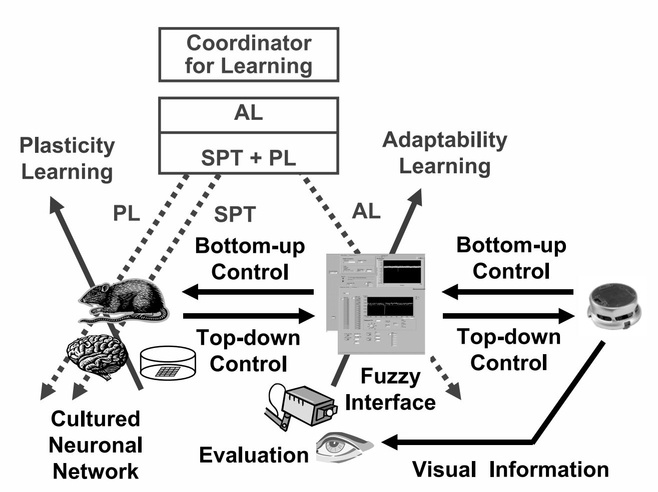

Fig. 8. Fuzzy Bio-Robot System

Figure 9 shows how to control a robot with living neuronal networks via fuzzy logic. We designed closed loop in which the robot of Khepera II receives the rotation speed of actuator in [-20, 20] from FLTD for eight inputs of patterns in multi-electrode array. Additionally, the multi-electrode unit receives stimulation points from FLBU for eight IR sensors of the robot. We designed 256 fuzzy rules with eight inputs and two output in FLBU and FLTD, respectively.

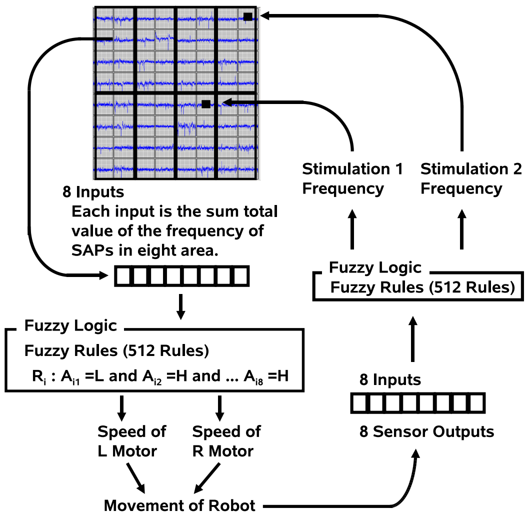

Fig. 9. Robot Control with Living Neuronal Network

Now, we explain how to design fuzzy rules in FLTD. First, we divide 64 electrodes in eight parts as inputs for FLTD, and define two kinds of membership functions of "High" and "Low" potentials in each part of electrodes. Thus, we become to constitute 256 fuzzy rules. Two electrodes are arbitrarily seleceted as stimulus points, and we detect the potential response for the first stimulus from other 62 electrodes. The pulse pattern of potential responses is input to the antecedent part of fuzzy rules, and the membership value of each rule is calculated. Next, we detect the pulse pattern of potential responses for the second stimulus, and also calculate the membership value of each rules. For two different membership values, we calculate the subtraction between them and assign motor speed of robot actuators to rules whose differentials are large. We additionally adjust the value of motor speed better with the steepest descent method. If the neuronal networks have regularity of logical potential response, the robot will be controlled well.

To demonstrate the regularity of neuronal networks, we applied the fuzzy bio-robot system to the straight running. We estimate if the Khepera robot can run straight in a track without bumping into a wall. The running track is the length of 120mm and the width of 90mm. Figure 10 shows the running track.

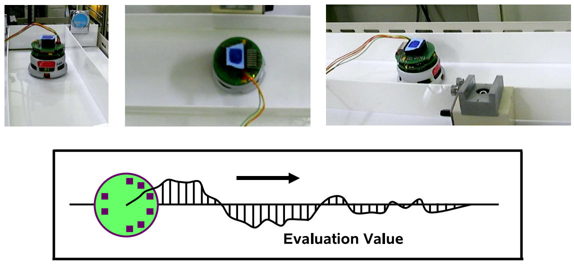

Fig. 10. Experimental Course

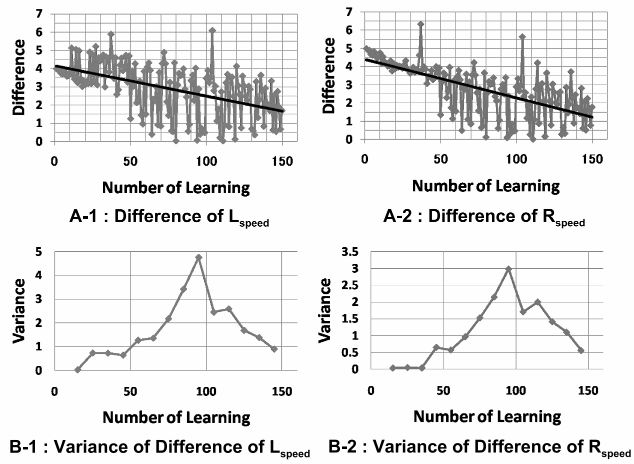

Fig. 11. Learning of Fuzzy Rule

The deviation between the output of FLTD and target output is shown in the part A of Figure 11. The variance of each 10 times of learning is shown in the part B. The deviation is gradually decreasing according to the number of learning. Actually, the deviation of the left actuator, L_{speed}, decreased by 40.3% for 50 learning times and become 1.673. The deviation of the right actuator, R_{speed}, decreased by 27.8% and become 1.224.

Next, we show the motor speed, the subtraction $L_{speed} - R_{speed}$ and $R_{speed} - L_{speed}$ of each fuzzy rule in Figure 12.

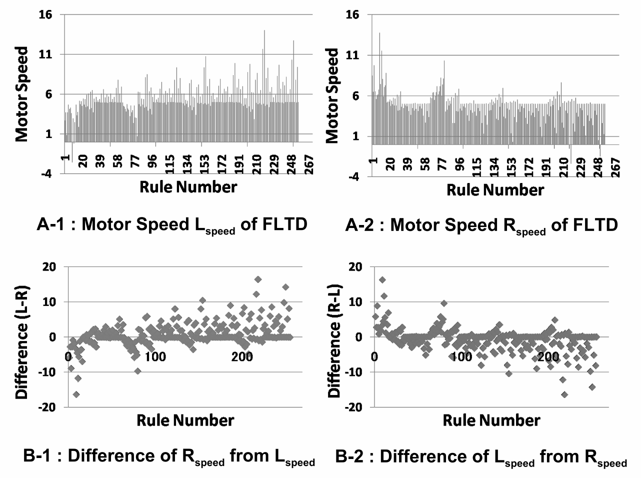

Fig. 12. Consequent Motor Speed of Fuzzy Rule

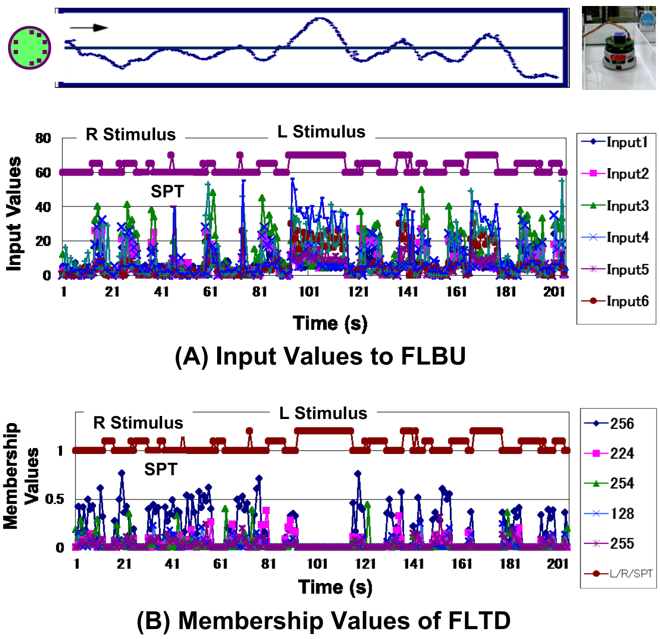

Fig. 13. Trace of Khepera Robot and Membership Values of FLTD

We should notice that the control values to turn on the right are assigned to the consequent part of the higher number of fuzzy rules because of the large deviation of $L_{speed} - R_{speed}$. The control values to turn on the left should be also assigned to the consequent part of the lower number of fuzzy rules because of the large deviation of $R_{speed} - L_{speed}$.

We next monitored the membership value of fuzzy rules fired while the robot is running in a track under condition of $1mM$ density of Mg_2^+. Figure 13 shows a trajectory of the robot running and the membership values in FLTD. The part A shows the changing of sensor value detected with Khepeara. The part B shows the membership values in FLTD. The Khepera II robot could run in a straight without bumping on the wall. In the part A, we monitored two high frequency pulses of “Input 4” for “L Stimulus”, and “Input3” for “R Stimulus”. In the part B, we detected the high membership value in the 256th fuzzy rule whose membership functions are all “Low” potentials. That is, the Khepera robot is usually running in a straight with spontaneous action potentials with the 256th fuzzy rule, however the specific fuzzy rules to avoid collision with wall are fired when the Khepera was too close to wall.

To discuss the fuzzy rules to avoid collision with wall in more detail, we monitored fuzzy rules whose membership values are relatively higher until $40s$ in Figure 14. In the part A, the Khepera robot detects the wall in the left side, and turns on the right with the 13th and 14th fuzzy rules, or the 15th and 16th fuzzy rules, simultaneously. The specificity of these fuzzy rules pattern appears regularly. In other words, the neuronal networks have regularity of logical potential response.

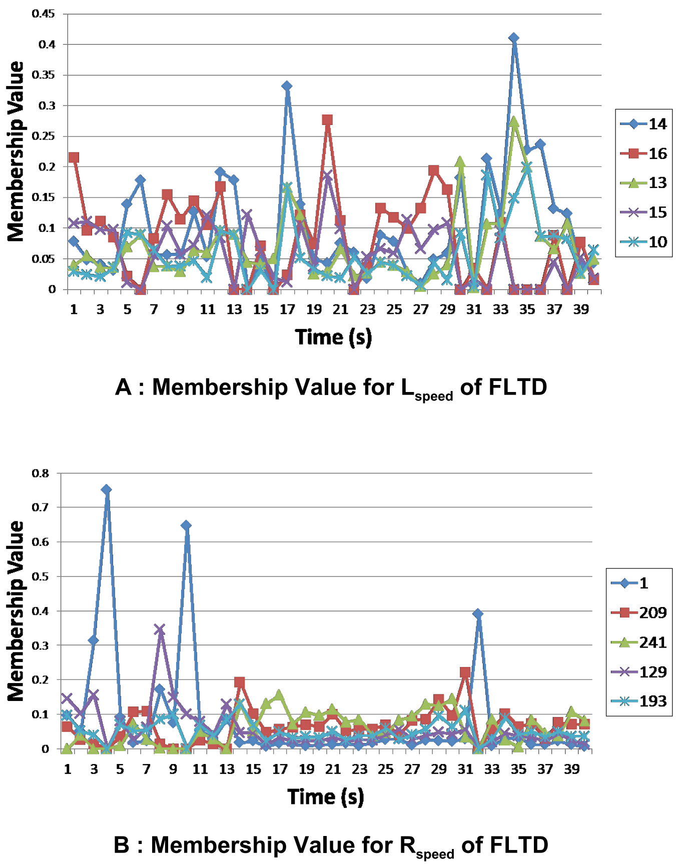

Fig. 14. Membership Values of FLTD until 40s

Finally, we observed the trajectory of the Khepera with camera placed above of the track course. We image a base line drawning along the centerline of the track course from the start position of the Khepera. We detected the deviation between the base line and the trajectory of the Khepera, and defined absolute value of the deviation as evaluation value. Figure 15 shows a change of the evaluation for running trials of iteration. The evaluation values decrease as running trials of iteration, and the Khepera became to run along the base line. We conclude that the decreasing will be due mainly to learning of neuronal networks.

In addition, we calculated the rate of the Khepera completed the course in 20 trials in Table II. The completed courses were 16 times, and the case of the Khepera crashed on the wall and stopped were four times. However, the rate of completed the course is high with 80%. We conclude that the logicality of neuronal networks and the adaptability of the fuzzy logic work efficiently. We should also conclude that the rate 80% is extremely high because of living neuronal networks.

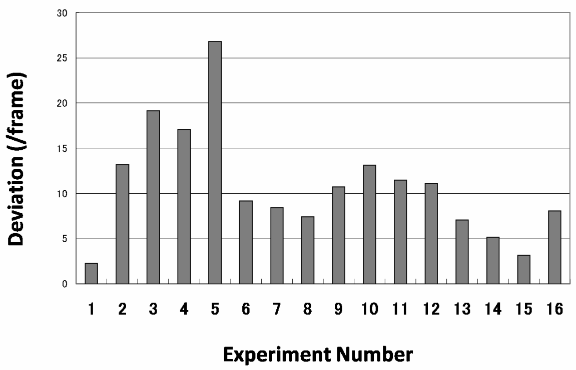

Fig. 15. Trace Deviation of Khepera Robot

TABLE II

COMPLETED RUN RATE OF KHEPERA ROBOT

	Experiment Number	Rate
Completed Run	1,3,4,5,6,7,8,9,10,14 15,16,17,18,19,20	80.0%
Incompleted Run	2,11,12,13	20.0%

VI. CONCLUSION

In this paper, we discussed acquiring a logicality of living neuronal network with data method of fuzzy connective operator, and applying fuzzy bio-interface to control fuzzy bio-robot. We should discuss the relationship between learning of living neuronal networks and adaptability of fuzzy logic more deeply in the near future.

REFERENCES

[1] S.N.Kudoh and T.Taguchi, "Operation of spatiotemporal patterns stored in living neuronal networks cultured on a microelectrode array," *Advanced Computational Intelligence and Intelligent Informatics*, Vol.8, No2, pp.100-107, 2003.

[2] S.N.Kudoh, R.Nagai, K.Kiyosue, and T.Taguchi, "PKC and CaMKII dependent synaptic potentiation in cultured cerebral neurons," *Brain Research*, Vol.915, No11 pp.79-87, 2001.

[3] L.M.A.Bettencourt, G.J.Stephens, M.I.Ham, and G.W.Gross, "Functional structure of cortical neuronal networks grown in vitro," *Phisical Review*, Vol.75, p.02915, 2007.

[4] I.Hayashi, E.Naito, and N.Wakami, "Proposal for fuzzy connectives with a learning function using the steepest descent method," *Japanese Journal of Fuzzy Theory and Systems*, Vol.5, No.5, pp.705-717, 1993.

[5] B.Schweizer and A.Sklar, "Associative functions and statistical triangle inequalities," *Publicationes Mathematicae Debrecen*, Vol.8, pp.169-186, 1961.

[6] S.N.Kudoh, I.Hayashi, and T.Taguchi, "Synaptic potentiation re-organized functional connections in a cultured neuronal network connected to a moving robot," *Proc. of the 5th International Meeting on Substrate-Integrated Micro Electrode Arrays (MEA2006)*, pp.51-52, Reutlingen, Germany in July 4-7, 2006.

[7] S.N.Kudoh, T.Taguchi, and I.Hayashi, "Interaction and intelligence in living neuronal networks connected to moving robot," *Proc. of 2006 IEEE International Conference on Fuzzy Systems (FUZZ-IEEE2006) in 2006 IEEE World Congress on Computational Intelligence (WCCI2006)*, pp.6271-6275 (No.FUZZ4516), Vancouver, Canada in July 16-21, 2006.

[8] I.Hayashi, T.Taguchi, and S.N.Kudoh, "Biomodeling system by living neuronal network connected to moving robot," *Proc. of International Symposium on Artificial Brain with Emotion and Learning (ISABEL2006)*, pp.164-165, Seoul, Korea in August 24-25, 2006.

[9] I.Hayashi, T.Taguchi, and S.N.Kudoh, "Learning and memory in living neuronal networks connected to moving robot, *Proc. of 8th International Symposium on advanced Intelligent Systems (ISIS2007)*, pp.79-81, Sokcho, Korea in September 5-8 (2007).

[10] S.N.Kudoh, C.Hosokawa, A.Kiyohara, T.Taguchi, and I.Hayashi, "Biomodeling system - Interaction between living neuronal network and outer world," *Journal of Robotics and Mechatronics*, Vol.19, No.5, pp.592-600, 2007.

[11] Y.Tsukamoto, "Fuzzy Sets as a Interface between Language Model and Mathmatics Model," *Proc of the 24th Fuzzy System Symposimu*, Vol.251-254, 2008.

[12] D.J.Bakkum, A.C.Shkolnik, G.Ben-Ary, P.Gamblen, T.B.DeMarse, and S.M. Potter, "Removing some 'A' from AI: Embodied cultured networks," in *Embodied Artificial Intelligence*, editered by F.Iida, R.Pfeifer, L.Steels, and Y.Kuniyoshi, New York, Springer, pp.130-145, 2004.

[13] Z.C.Chao, D.J.Bakkum, and S.M. Potter, "Shaping embodied neural networks for adaptive goal-directed behavior," *PLoS Comput Biol*, Vol.4, No.3, p.e1000042, 2008.

[14] K.Warwick: Implications and consequences of robots with biological brains, *Journal of Ethics and Information Technology*, Vol.12, No.3, pp.223-234 (2010).

[15] T.B.DeMarse and K.P.Dockendorf: Adaptive Flight Control with Living Neuronal Networks on Microelectrode Arrays, *Proc. of 2005 IEEE International Joint Conference on Neural Networks (IJCNN2005)*, pp.1549-1551, Montreal, Canada (2005).

[16] D.Xydas, D.J.Norcott, K.Warwick, B.J.Whalley, S.J.Nasuto, V.M.Becerra, M.W.Hammond, J.Downes, and S.Marshall: Architecture for Neuronal Cell Control of a Mobile Robot, in *European Robotics Symposium 2008*, editored by H.Bruyninckx, L.Preucil, and M.Kulich, Springer, Vol.44, pp23-31 (2008).

[17] P.Marks: Rat-brained Robots take Their First Steps, *New Scientist*, Vol.199, No.2669, pp.22-23 (2008).

[18] I.Hayashi, M.Kiyotoki, A.Kiyohara, M.Tokuda, and S.N.Kudoh, "Acquisition of Logicality in Living Neuronal Networks and its Operation to Fuzzy Bio-Robot System," *Proc. of 2010 IEEE International Conference on Fuzzy Systems (FUZZ-IEEE2010) in 2010 IEEE World Congress on Computational Intelligence (WCCI2010)*, pp.543-549, 2010.